

Semantics-Aware Image to Image Translation and Domain Transfer

Pravakar Roy
University of Minnesota
Minneapolis, MN, USA
royxx268@umn.edu

Nicolai Häni
University of Minnesota
Minneapolis, MN, USA
haeni001@umn.edu

Volkan Isler
University of Minnesota
Minneapolis, MN, USA
isler@umn.edu

Abstract

Image to image translation is the problem of transferring an image from a source domain to a target domain. We present a new method to transfer the underlying semantics of an image even when there are geometric changes across the two domains. Specifically, we present a Generative Adversarial Network (GAN) that can transfer semantic information presented as segmentation masks. Our main technical contribution is an encoder-decoder based generator architecture that jointly encodes the image and its underlying semantics and translates both simultaneously to the target domain. Additionally, we propose *object transfiguration* and *cross domain semantic consistency* losses that preserve the underlying semantic labels maps. We demonstrate the effectiveness of our approach in multiple object transfiguration and domain transfer tasks through qualitative and quantitative experiments. The results show that our method is better at transferring image semantics than state of the art image to image translation methods.

1 Introduction

What does it take for a computer to convert an image of a horse into an image of a zebra, or a photograph into a painting created by one of the masters of the Renaissance? Humans have no difficulty imagining such a transformation by changing the style, color or even geometry of objects while keeping the underlying semantics of the scene intact. In this paper, we study this problem of capturing the composition of a set of images and changing these characteristics, while keeping the semantics of the scene consistent.

The task of finding a mapping to translate images from a source domain to a target domain is known as *image to image translation*. Many problems in computer vision and computer graphics can be posed as a translation task. Semantic segmentation [2], image synthesis [3], image coloring [4] and image super-resolution [5] are all examples where we try to find an intrinsic mapping between two related domains. Years of research have produced a variety of algorithms to tackle this problem when data pairing the

images from the two domains is available [2,3,6,7]. However, obtaining such paired data requires extensive annotation efforts, which are time-consuming and expensive.

Unsupervised image to image translation makes the collection of such image pairs unnecessary. The goal of unsupervised image to image translation is to estimate a mapping F from a source domain X to a target domain Y , based on independently sampled data instances $x_i \in X$ and $y_i \in Y$, such that the distribution of the mapped instances $F(x_i)$ matches the probability distribution P_y of the target domain. Generative Adversarial Networks (GANs) [8] have emerged as powerful image transformers. These networks treat image-to-image translation as an adversarial process, where two models are trained simultaneously: A generator representing the mapping $F : X \rightarrow Y$, and a discriminator D_y that estimates a probability of the sample being generated from the training data instead of F . Using variations of this approach, recent work has produced visually appealing results for mapping realistic photos to paintings [1,9,10], semantic segmentation maps to photos [11,12], and single image super-resolution [5].

State-of-the-art image to image translation methods fail when the mapping function includes significant geometric changes [1]. For example, if the transformation requires mapping squares to skinny triangles. This failure is because these methods do not take the underlying representation of the scene into consideration, and therefore make arbitrary changes to the appearance and geometry of the input. While this approach can be acceptable for image style transfer for artistic purposes, it is insufficient when the relationship between an image and its semantic labels needs to be preserved - such as in the case of domain adaptation or semantic segmentation. In this paper, we show that by preserving the class labels during the translation process we can improve the performance of existing semantic segmentation networks and generate qualitatively improved outputs. Toward this goal, we present a method that can leverage semantic class label maps. We present *SemGAN*, an encoder-decoder based generator architecture that can translate both the input image and corresponding semantic label map to the target

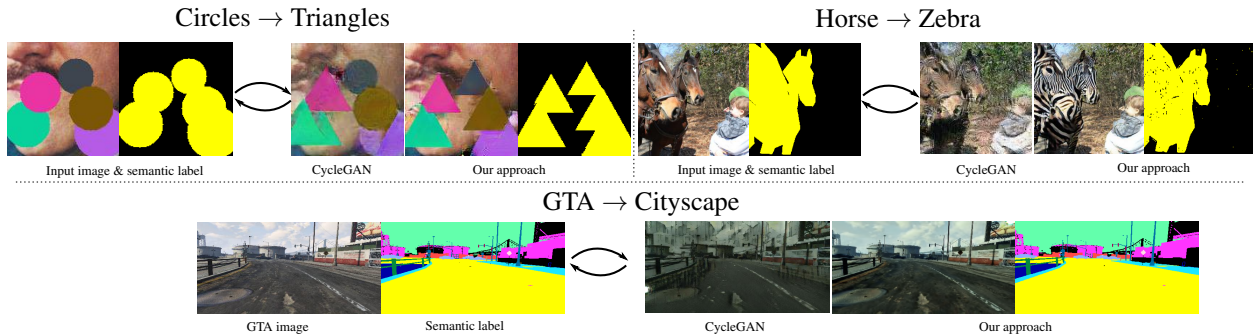


Figure 1: Given two unpaired image collections and semantic label masks, our network learns a mapping to translate images from one domain to the other while preserving the labels. Top left: Object transfiguration task for circles to triangles. Top right: Image to image style transfer from Horses to Zebras. Bottom: Domain translation from synthetic GTA to Cityscapes photos. The examples show the CycleGAN [1] output, the image and mask outputs of our method. Note that CycleGAN does not output masks.

domain simultaneously. The generator is divided into an encoder to jointly encode image and class information and two decoders to generate the target image and class labels. The discriminator operates on the joint encoding of the image and class labels. For object transfiguration tasks, we propose an additional loss term that encourages image background preservation.

2 Related Work

Generative Adversarial Networks (GAN’s) [8] have produced high-quality results on a variety of tasks. These type of network has been used extensively for image to image translation, both in a supervised [2, 3, 6, 7] and unsupervised [1, 9, 13–17] fashion. The key to their success is the inclusion of an adversarial loss, which drives the generator part of the network to create indistinguishable samples to the target distribution. After CycleGAN [1] introduced a cyclic consistency term to avoid mode collapse most new approaches have also adopted this cyclic consistency loss.

Extension of CycleGAN using Semantic Information The idea to use semantic consistency to translate between the source domain and target domain has been explored before us. Li *et al* [18] extended the CycleGAN framework with a Sobel filter loss. The Sobel filter is convolved with the semantic label in the source domain and the translated image to preserve the semantic boundaries between them. Ramirez *et al* [19] proposed to extend the discriminator network of CycleGAN to contain a classification and semantic segmentation network. The segmentation network is trained ahead of time and is integrated into the discriminator during the training stage. This idea of using a tasks specific network, either for classification or semantic segmentation, can also be found in Cycada [20].

Here, the network adds a task-specific loss to penalize semantic inconsistencies between the translated image and the source image. Sem-GAN [21] proposed two semantic segmentation functions that are trained on the respective domains. The output of the generator is used as input to this semantic segmentation function which again penalizes semantic inconsistency. In contrast to our proposed method, these works rely heavily on the introduction of sizeable semantic segmentation networks, which is computationally expensive. Additionally, they restrict the geometric changes that a network is allowed to perform. When a translation requires substantial geometric changes, as in $Cat \rightleftharpoons Dog$ or $Sheep \rightleftharpoons Giraffe$, this is not desirable.

Object Transfiguration and Semantic Manipulation Most of the image to image translation methods discussed so far are only capable of modifying low-level content of images, such as transferring colors or textures. They fail to perform large semantic changes between objects (*e.g.* $token \rightarrow transform$ sheep into giraffes). This failure is due to the underlying assumption that the scenes and the contained objects are similar in geometric composition across both domains. Others have focused on using GAN’s for object transfiguration and semantic manipulation. One proposed method [22] is to optimize a conditional generator and several semantic-aware discriminators. Another idea [23] relied on modeling an attention map to extract the foreground objects. Instead of considering the whole image in the transfiguration task, the generator is restricted to the foreground objects. InstaGAN [24] proposed to use instance level segmentation masks in both, the source and the target domains. Each of the generator and discriminator networks receives an image and a set of instance masks, which are then translated one by one. To preserve the background, they introduce a context preservation loss.

In this paper, we show that we can obtain superior performance on the object transfiguration task using only a slight modification to the original CycleGAN approach. We present an encoder-decoder based generator architecture that can translate both the input image and corresponding semantic map to the target domain in a single forward pass of the network.

Domain Adaptation

In general, networks trained on a source domain and tested on a target domain will perform poorly, even if the two domains appear visually similar to an outside observer. Domain adaptation tries to bridge this gap. This topic has been extremely popular in the last few years [20, 25–31]. While these approaches can translate from one image domain to another, the underlying semantics are lost if the network is allowed to manipulate an object’s geometry. In this work, we show that we can perform domain adaptation while preserving these semantic label maps.

3 Semantic-Aware GAN

Given, two image domains \mathcal{X}, \mathcal{Y} , and unpaired training samples $\{x_i\}_{i=1}^N, \{y_j\}_{j=1}^M$ where $x_i \in \mathcal{X}, y_j \in \mathcal{Y}$, unsupervised image to image translation aims to learn a mapping $F : \mathcal{X} \rightarrow \mathcal{Y}$ between the two domains. Let x, y denote the sample distributions from \mathcal{X}, \mathcal{Y} (i.e $x \sim p_{data}(\mathcal{X}), y \sim p_{data}(\mathcal{Y})$). The goal of the mapping is to fool an adversarial discriminator D_Y so that it cannot distinguish between $\{F(x)\}$ and $\{y\}$. In other words, the objective of the mapping is to fool the discriminator into thinking that $F(x) \sim p_{data}(\mathcal{Y})$.

In this work, we extend the formulation of unsupervised image to image translation to contain semantic information as well. Our goal is to learn a transfer function to jointly translate an image and its underlying semantics. Let each image in domains \mathcal{X} and \mathcal{Y} be associated with a class map \mathcal{C}_X and \mathcal{C}_Y , where each pixel in these class maps belongs to one and only one of the classes C_1, \dots, C_k . Accordingly, their joint distributions can be represented by $(\mathcal{X} \times \mathcal{C}_X)$ and $(\mathcal{Y} \times \mathcal{C}_Y)$. Given independently sampled images and corresponding class labels $\{x_i, c(x_i)\}_{i=1}^N, \{y_j, c(y_j)\}_{j=1}^M$ where $(x_i, c(x_i)) \in (\mathcal{X} \times \mathcal{C}_X), (y_j, c(y_j)) \in (\mathcal{Y} \times \mathcal{C}_Y)$, our goal is to learn a transfer function $F : (\mathcal{X} \times \mathcal{C}_X) \rightarrow (\mathcal{Y} \times \mathcal{C}_Y)$ that fools an adversarial discriminator D_Y , presuming $\{F(x, c(x))\} \sim p_{data}(\mathcal{Y} \times \mathcal{C}_Y)$. Our objective contains the standard adversarial and cycle-consistency loss proposed by [1, 8] and we add task specific losses for *object transfiguration* and *cross domain semantic consistency*.

3.1 Sem-GAN Architecture:

The GAN formulation is a two network minimax game. The generator (F) is trying to minimize $D_Y(F(x, c(x)))$ -the probability of the generated samples being adjudicated fake by the discriminator. At the same time, the discriminator D_Y is trying to maximize the probability of detecting the real samples $D_Y(y, c(y))$.

For the generator F we use an encoder-decoder architecture. F consists of three networks - an encoder F_E which jointly encodes the image and underlying semantics, a decoder F_{D_x} for generating the image and another decoder F_{D_c} for generating the semantic labels. The discriminator is a single network that encodes the image and class labels jointly, outputting the probability of the sample under observation being real.

Optimizing this adversarial objective is difficult and can lead to mode collapse (all inputs are mapped to a single output) [8]. To avoid this problem, CycleGAN [1] proposed a cyclic consistency loss. In cyclic consistency, two mappings $F(\mathcal{X} \rightarrow \mathcal{Y})$ and $G(\mathcal{Y} \rightarrow \mathcal{X})$ are learned simultaneously. Enforcing this cyclic consistency encourages $(F(G(x)) \approx x$ and $G(F(y)) \approx y)$, adds more structure to the objective and avoids mode collapse. We leverage this approach while building Sem-GAN. We train two coupled mappings $F : (\mathcal{X} \times \mathcal{C}_X) \rightarrow (\mathcal{Y} \times \mathcal{C}_Y)$, $G : (\mathcal{Y} \times \mathcal{C}_Y) \rightarrow (\mathcal{X} \times \mathcal{C}_X)$ and two discriminators D_X, D_Y simultaneously. To align the joint distribution of the images and underlying semantics of source and target domain, the cycle loss terms are augmented with task specific losses.

3.2 Adversarial Loss

The GAN framework is a minimax game where the discriminator plays the adversarial role by distinguishing between samples of the target distribution and the ones being produced by the generator. We apply the standard adversarial loss for GAN networks [8] to both mappings. For the mapping $F : \mathcal{X} \times \mathcal{C}_X \rightarrow \mathcal{Y} \times \mathcal{C}_Y$ the loss is expressed as:

$$\begin{aligned} \mathcal{L}_{Adv}(F, D_Y, \mathcal{X} \times \mathcal{C}_X, \mathcal{Y} \times \mathcal{C}_Y) = & \mathbb{E}_{(y, c(y)) \sim p_{data}(\mathcal{Y} \times \mathcal{C}_Y)} [\log(D_Y(y, c(y)))] \\ & + \mathbb{E}_{(x, c(x)) \sim p_{data}(\mathcal{X} \times \mathcal{C}_X)} [1 - \log(D_Y(F(x, c(x))))] \end{aligned} \quad (1)$$

F tries to minimize this objective by generating images and semantic labels $F(x, c(x))$ that look similar to instances from the target domain. Simultaneously, D_Y strives to maximize this objective to distinguish between the generated samples and the real ones. This leads to the optimization objective: $\min_F \max_{D_Y} \mathcal{L}_{Adv}(F, D_Y, \mathcal{X} \times \mathcal{C}_X, \mathcal{Y} \times \mathcal{C}_Y)$. Similarly, for the mapping G we define the objective as $\min_G \max_{D_X} \mathcal{L}_{Adv}(G, D_X, \mathcal{Y} \times \mathcal{C}_Y, \mathcal{X} \times \mathcal{C}_X)$.

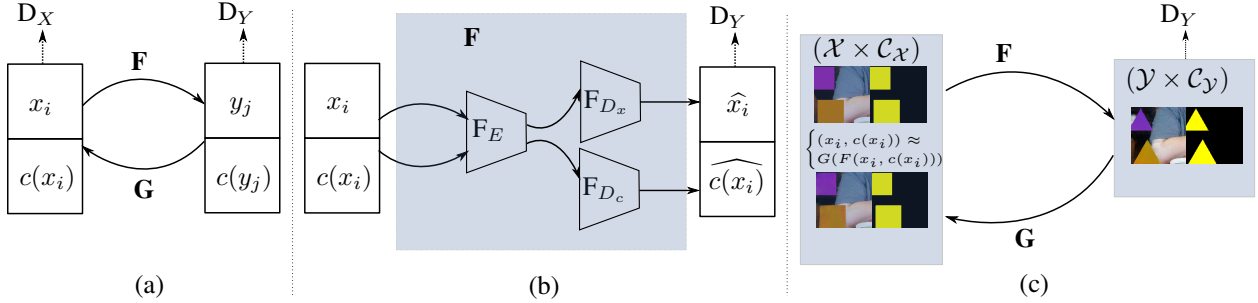


Figure 2: (a) Our model learns two mapping functions $F : (\mathcal{X} \times \mathcal{C}_X) \rightarrow (\mathcal{Y} \times \mathcal{C}_Y)$ and $G : (\mathcal{Y} \times \mathcal{C}_Y) \rightarrow (\mathcal{X} \times \mathcal{C}_X)$ together with the associated adversarial discriminators D_X and D_Y . D_X encourages F to translate images and masks to be indistinguishable from samples in domain $(\mathcal{Y} \times \mathcal{C}_Y)$ and vice versa for D_X and G . (b) We use an encoder F_E to encode the stacked image and the semantic map. The latent representations are decoded separately in F_{D_x} and F_{D_c} to get a translated representation $(\hat{x}_i, \hat{c}(x_i)) = F(x_i, c(x_i))$. (c) An example object transfiguration task where our network translates squares into triangles while preserving the background and maintaining the consistency between the mask and the image.

3.3 Cycle Consistency Loss

To add additional structure to our objective, we enforce cyclic consistency following CycleGAN [1]. CycleGAN enforces consistency across the two mappings f, G using L_1 norm between the original and the reconstructed image $\|G(F(x)) - x\|_1$. As our formulation includes images as well as semantic labels we need to account for the classification loss as well. We define the standard cross-entropy loss for multi-class classification as:

$$\mathcal{C}(C_X, t_x, c(x)) = - \sum_{k=1}^{C_X} \mathbb{1}_{k=t_x} \log c(x) \quad (2)$$

where, C_X is the total number of classes, t_x is the ground truth class label and $c(x)$ is the predicted outcome. Let $F(x, c(x)) = (\hat{y}, \hat{c}_y)$, $G(\hat{y}, \hat{c}_y) = (\hat{x}, \hat{c}_x)$ and $G(y, c(y)) = (\hat{x}, \hat{c}_x)$, $F(\hat{x}, \hat{c}_x) = (\hat{y}, \hat{c}_y)$. Given this we can define cyclic consistency across images and semantic labels as:

$$\begin{aligned} \mathcal{L}_{Cyc}(F, G) = & \mathbb{E}_{(x, c(x)) \sim p_{data}(\mathcal{X} \times \mathcal{C}_X)} [\|x - \hat{x}\|_1 \\ & + \mathcal{C}(C_X, c(x), \hat{c}_x)] + \mathbb{E}_{(y, c(y)) \sim p_{data}(\mathcal{Y} \times \mathcal{C}_Y)} [\|y - \hat{y}\|_1 \\ & + \mathcal{C}(C_Y, c(y), \hat{c}_y)] \end{aligned} \quad (3)$$

3.4 Object Transfiguration Loss

For many object transfiguration tasks (such as from triangle to circles), it is intuitive that the color component of the translated objects and the background are preserved. To enforce similar color composition we follow [1, 13] and add an *identity loss* term \mathcal{L}_{Idt} to our objective. This term encourages the generator to be an identity mapping when samples of the target domain are provided as input.

Let $F(y, c(y)) = (\hat{y}, \hat{c}_y)$ and $G(x, c(x)) = (\hat{x}, \hat{c}_x)$. With this notation, we define the identity loss as:

$$\begin{aligned} \mathcal{L}_{Idt}(F, G) = & \mathbb{E}_{(y, c(y)) \sim p_{data}(\mathcal{Y} \times \mathcal{C}_Y)} [\|y - \hat{y}\|_1 \\ & + \mathcal{C}(C_Y, c(y), \hat{c}_y)] + \mathbb{E}_{(x, c(x)) \sim p_{data}(\mathcal{X} \times \mathcal{C}_X)} [\|x - \hat{x}\|_1 \\ & + \mathcal{C}(C_X, c(x), \hat{c}_x)] \end{aligned} \quad (4)$$

To preserve the background or other semantic elements in the image we introduce a *class preserving loss*. Let c be the number of semantic categories we want to translate and $W_x, W_{\hat{y}}$ be the corresponding semantic pixel masks for these categories in the source and translated image. Then $W_{x\hat{y}} = \overline{W_x \cup W_{\hat{y}}}$ represents a pixel-map where the source and translated image have similar content. Let $F(x, c(x)) = (\hat{y}, \hat{c}_y)$ and $G(y, c(y)) = (\hat{x}, \hat{c}_x)$. Assuming this masks are denoted by $W_{x\hat{y}}, W_{y\hat{x}}$ for F, G , we define the class preserving loss as:

$$\begin{aligned} \mathcal{L}_{Cls}(F, G) = & \mathbb{E}_{(x, c(x)) \sim p_{data}(\mathcal{X} \times \mathcal{C}_X)} W_{x\hat{y}} \odot [\|x - \hat{y}\|_1] \\ & + \mathbb{E}_{(y, c(y)) \sim p_{data}(\mathcal{Y} \times \mathcal{C}_Y)} W_{y\hat{x}} \odot [\|y - \hat{x}\|_1] \end{aligned} \quad (5)$$

3.5 Cross-Domain Semantic Consistency Loss

For domain translation applications it is desired that the underlying geometry of the environment is preserved in the translation process. To encourage preserving geometry in such cases we add a *cross domain semantics preservation loss* term to our objective. Let $F(x, c(x)) = (\hat{y}, \hat{c}_y)$ and $G(y, c(y)) = (\hat{x}, \hat{c}_x)$. We define the cross-domain semantic consistency term as:

$$\begin{aligned} \mathcal{L}_{Sem}(F, G) = & \mathbb{E}_{(x, c(x)) \sim p_{data}(\mathcal{X} \times \mathcal{C}_X)} [\mathcal{C}(C_X, c(x), \hat{c}_y)] \\ & + \mathbb{E}_{(y, c(y)) \sim p_{data}(\mathcal{Y} \times \mathcal{C}_Y)} [\mathcal{C}(C_Y, c(y), \hat{c}_x)] \end{aligned} \quad (6)$$

3.6 The Objective Function

Our full objective is:

$$\begin{aligned} \mathcal{L}(F, G, D_X, D_Y) = & \mathcal{L}_{Adv}(F, D_Y, \mathcal{X} \times \mathcal{C}_X, \mathcal{Y} \times \mathcal{C}_Y) + \\ & \mathcal{L}_{Adv}(G, D_X, \mathcal{Y} \times \mathcal{C}_Y, \mathcal{X} \times \mathcal{C}_X) + \lambda_{Cyc} \mathcal{L}_{Cyc}(F, G) + \\ & \lambda_{Idt} \mathcal{L}_{Idt}(F, G) + \lambda_{Cls} \mathcal{L}_{Cls}(F, G) + \\ & \lambda_{Sem} \mathcal{L}_{Sem}(F, G) \end{aligned} \quad (7)$$

, where λ controls the relative importance of the different losses. Our target is to solve:

$$G^*, F^* = \arg \min_{G, F} \max_{D_X, D_Y} \mathcal{L}(G, F, D_X, D_Y) \quad (8)$$

In Section 5 we compare our method against ablations of full objective.

4 Implementation

Network Architecture Our implementation is based on the PyTorch [32] version of CycleGAN [1]. In particular, we used building blocks from the ResNet 9-blocks generator. Our generator contains downsampling and residual blocks in the encoder and upsampling and residual blocks in the decoders. Many previous implementations used standard deconvolution layers which lead to checkerboard effects (Figure 3, column 3). We replace the deconvolution layers with upsampling layers and regular convolutions. We stacked the images and semantic maps together as network inputs. Prior to stacking, the semantic maps were converted to one-hot encoding and normalized to the same range as the images ($[-1, 1]$). As a result, the dimension of our input varies depending on the total number of classes in a particular domain. For an image with dimension, $m \times n$ and number of classes k the dimension of the input is $m \times n \times k$. For the activation layers of the two decoders (image and semantic labels), we used tanh and soft-max non-linearities respectively.

For the discriminator, we used the 70×70 PatchGAN [6] network. Again, for input to the discriminator, we stacked the images and semantic maps together with proper normalization.

Training Details and Parameters All networks used in this work were trained on a single machine containing two NVIDIA Tesla K20X GPUs, each with 12 GB of memory. We used Adam optimizer with the same initial learning rate of 0.0002. The discriminator was trained

with a history of the last 50 images. We applied Instance Normalization to both the generator and discriminator and for all the experiments, the networks were trained up to 200 epochs. For object transfiguration tasks, λ_{Sem} was set to zero to remove cross domain consistency. Similarly, for domain translation tasks λ_{Cls} was set to zero to turn off class preserving loss. We used $\lambda_{Cyc} = 10, \lambda_{Idt} = 10$ for all the experiments.

Similar to CycleGAN, we replace the negative log-likelihood term in \mathcal{L}_{Adv} ((1)) with a least square loss.

5 Results

We study the effectiveness of our approach for several object transfiguration and domain translation tasks. For image to image translation, we compare our approach to two state-of-the-art techniques (CycleGAN [1], InstaGAN [24]) at the task of translating simple geometric shapes with arbitrary background and color. For domain translation, we compare our approach both qualitatively and quantitatively against CycleGAN. In addition, we conduct qualitative and quantitative ablation studies for both these tasks. The PyTorch code, models and data will be made available on our project website upon publication.

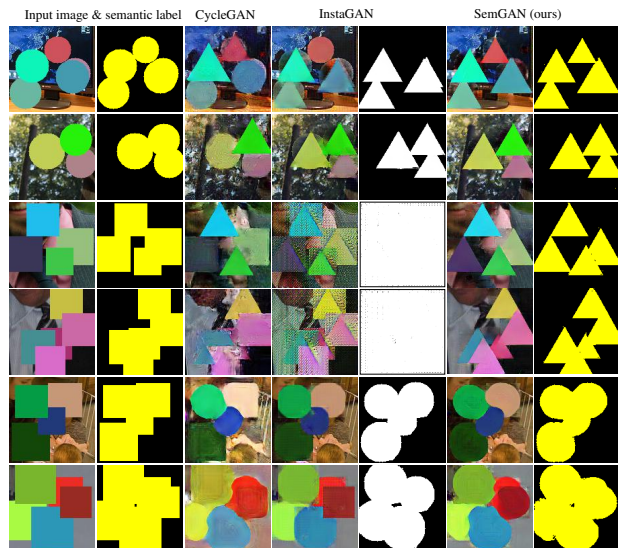


Figure 3: Qualitative comparison of CycleGAN, InstaGAN and our method on the task of transforming circles into triangles (top two rows), squares into triangles (center two rows) and squares into circles (bottom two rows). InstaGAN translation of the label masks in the Squares \rightarrow Triangle case (center rows) leads to mode collapse.

5.1 Object Transfiguration Results

For image to image translations that involve significant geometric changes, we create a simple shapes dataset, by overlaying basic geometric shapes (circle, triangle, and square) on randomly chosen images from the COCO [33] dataset. Each dataset contains a random number (1 – 10) of one type of geometric object. Each network has to transform all foreground objects in the image another category (e.g Circle→ Triangle). The goal is to only change the shape and keep the original color composition and image background intact. We created three of these datasets for circles, triangles, and squares. Each dataset contains 1000 training images and 50 test images. Semantic and instance level information is available for all the datasets.

5.1.1 Baselines

CycleGAN [1] is a method for general purpose unpaired image to image translation that leverages cyclic consistency. Many image to image translation techniques, including ours follow the architecture of this method. It does not use any underlying semantic information.

InstaGAN [24] is a method for object transfiguration with instance level information. This approach has access to class label maps as well as instance information and should outperform our method. During our experiments, InstaGAN took an extremely long time to train and we could not finish training for the horse to zebra translation task.

Our approach outperforms CycleGAN on all datasets. As CycleGAN does not have any access to semantic information, it does not know which semantic objects to translate and often leaves the objects unchanged. Figure 3 (first row, column three) shows one such example. It is also inconsistent regarding background preservation. InstaGAN performs poorly on two out of the three datasets. For translation from Square ↔ Triangle, InstaGAN suffers from mode collapse. For the Square → Circle translation task, it performs comparably to our approach. Figure 3 shows a few qualitative comparisons.

Figure 4 compares our method to CycleGAN on the Horse ↔ Zebra transformation tasks. Our approach translates textures, colors, and geometry more consistently. This dataset was created using the same procedure as in [24]

In Figure 5 we present qualitative comparisons of ablations of our full objective. Removing the class preserving loss decreases the preservation of the background and the foreground object boundaries become more diluted. Removing the identity loss leaves the network to change the color of the objects and background and removing the cyclic consistency leads to artifacts in the foreground and background.

5.2 Domain Transfer Results

For domain transfer, we perform two sets of experiments. First, we transform red to green apples in orchard environments. With this experiment, we demonstrate the effectiveness of our approach quantitatively. Second, we perform synthetic → real domain translation experiments using the GTA [34] → Cityscape [35] dataset. For this



Figure 4: Image to image translation task. Top: Horse → Zebra. Bottom: Zebra → Horse. Adding a label preserving loss aids the preservation of background and the translations of color, texture and geometry of the foreground object.

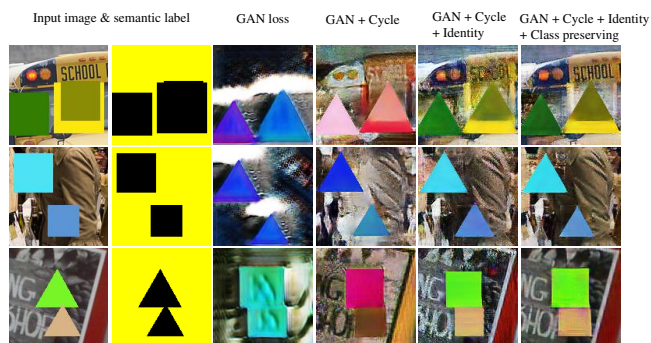


Figure 5: Object transfiguration ablation study: (Top two rows) Squares → Triangles and triangles → Squares.

experiment, we show a qualitative comparison of our method compared to CycleGAN.

5.2.1 Translation from Red to Green Apples

We translate between fruit trees in orchard settings, transforming red to green apples and vice versa. The dataset contains semantic information from both domains. Figure 6 shows example data and transfers. The goal of this experiment is to measure the effectiveness of using the translated data in training a semantic segmentation network.

Evaluation Metrics We adopt the Fully Convolutional Network (FCN) score metrics from [35] for quantitative evaluation. The FCN score evaluates the performance improvement when using translated images to train an off-the-shelf semantic segmentation network (*e.glet@tokeneonedotU-Net* [36]). The FCN predicts a semantic label map for an image which we compare to available ground truth data. If the translated images and labels are coherent and representative of the target domain, this should translate into higher FCN scores. On the other hand, any discrepancy between images and semantic labels will result in worse segmentation performance. To evaluate the performance we use the standard metrics from [35], namely mean pixel accuracy, mean class accuracy and mean class Intersection over Union (IoU).

Domain Adaptation Baselines **Target** network is trained on the training data in the target domain $(y_j, c(y_j))$. Since this data is trained on the same distribution as our test data, it represents an oracle whose performance we aim to attain with the other methods.

Source network is trained on the training data in the source domain $(x_i, c(x_i))$. Expectedly, this network will perform poorly when tested on the target domain due to the large domain gap.

Sem-GAN₅₀ uses all available data from the source domain $(x_i, c(x_i))$ and 50% of the translated data $(\hat{x}_i, \widehat{c}(x_i))$.

Sem-GAN₁₀₀ uses data from the source domain $(x_i, c(x_i))$ and 100% of the translated data $(\hat{x}_i, \widehat{c}(x_i))$.

To offer a fair comparison, we implement each of these networks using the same architecture and hyperparameters.

FCN Score We compare the networks label predictions to the available ground truth label maps. Table 2 and Table 1 report performance of the four methods. In both translation cases, adding our translated images to the test sets increases the performance when compared to the source only network. When adding all of the translated

images to the source data, the network even outperforms the Oracle network in most of the cases.

Loss	Pixel acc.	Class acc.	Class IoU
Source	0.89	0.51	0.46
Ours ₅₀	0.98	0.96	0.90
Ours ₁₀₀	0.98	0.97	0.91
Target	0.97	0.94	0.88

Table 1: Classification performance of Red → Green fruits

Loss	Pixel acc.	Class acc.	Class IoU
Source	0.91	0.50	0.47
Ours ₅₀	0.98	0.95	0.89
Ours ₁₀₀	0.99	0.98	0.95
Target	0.99	0.99	0.93

Table 2: Classification performance of Green → Red fruits

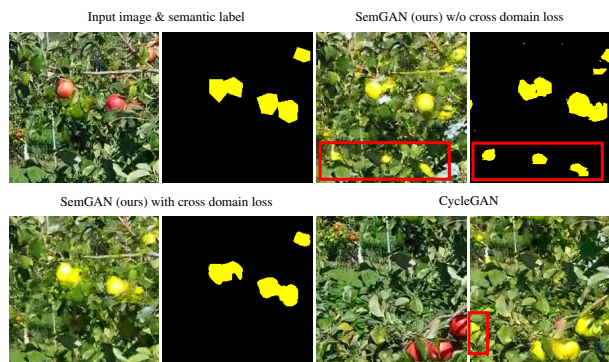


Figure 6: Domain transfer: red apples to green apples. We compare our network with and without cross domain preservation loss against CycleGAN. Our methods preserve the class labels, while CycleGAN adds fruits without changing the class label.

Table 3 and Table 4 show the ablation study on the Red → Green and Green → Red fruit translation task. We used the Target network from our FCN experiments as a noisy labeler and compare our translated label masks against the noisy labels. For CycleGAN, we make the assumption that the underlying semantics of the image is not changed by the translation. We find that using only cyclic consistency reduces performance. This confirms our initial suspicion, that unsupervised image to image translation does not preserve the underlying semantic labels. The results of Sem-GAN without the cross-domain loss outperform the ones with the cross-domain loss. Sem-GAN without the

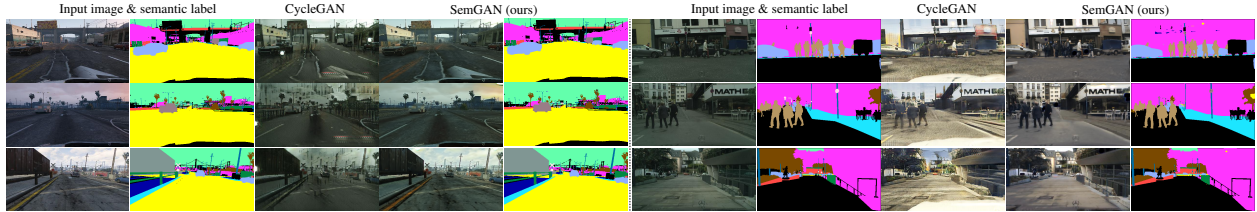


Figure 7: Domain transfer: $GTA \rightleftharpoons CityScape$. We show the performance of CycleGAN and our network (trained for only 66 epochs out of 200 due to time constraints. We will update this figure in the final paper). CycleGAN does not preserve underlying geometry and creates visual artifacts.



Figure 8: Variants of our network, trained with only partial or full class preservation. From left to right: Input image and semantic label, our network trained to preserve only classes [car, person, road] and our network trained to preserve all 19 classes. When only preserving a subset of the classes the network generates visual artifacts, similar to CycleGAN.

domain loss introduces apple like artifacts (See Figure 6 top row, rightmost) which are detected by the U-Net as apples. To discourage the network from producing such artifacts, we recommend using the cross-domain loss.

Loss	Pixel acc.	Class acc.	Class IoU
CycleGAN [1]	0.93	0.76	0.68
Sem GAN w.o cross domain loss	0.97	0.90	0.82
Sem GAN w cross domain loss	0.96	0.88	0.80

Table 3: Ablation study: Classification performance of red \rightarrow green fruit translation

Loss	Pixel acc.	Class acc.	Class IoU
CycleGAN [1]	0.93	0.84	0.66
Sem GAN w.o cross domain loss	0.93	0.90	0.82
Sem GAN w cross domain loss	0.94	0.86	0.73

Table 4: Ablation study: Classification performance of green \rightarrow red fruit translation

5.2.2 Qualitative Results on $GTA \leftrightarrow Cityscape$

One of the main advantages of our formulation is the ability to preserve semantic consistency throughout the translation process. However, for all the experiments so far our test cases only had singleton classes. In this experiment,

our goal is to test how our approach performs in the presence of multiple classes. Fig. 7 shows qualitative examples of translation from $GTA \rightarrow Cityscape$ and vice versa. Our approach produces more semantically consistent and visually appealing results compared to CycleGAN.

To understand how semantic information helps the translation process, we trained a variant of our network with access to only a subset of the underlying semantic information (people, cars, roads, and background). Figure 8 shows that the translated images from this network contain visual artifacts similar to CycleGAN (buildings merged into the sky).

6 Limitations and Discussion

In this work, we presented an unsupervised image to image translation network which can transfer semantic labels consistently. In object transfiguration tasks, the network preserved not only the class maps but also generated more detailed results on the image level. In the domain translation experiments, our method’s label preservation mechanism reduces visual artifacts. For example, in contrast to CycleGAN, we observed no random permutations of objects in the scene (changing vegetation to buildings, etc.). In the $GTA \rightarrow Cityscape$ experiment our cross-domain loss prevented similar failures from happening.

However, when there is a significant overlap between individual instances, the network sometimes produced visual artifacts as shown in Figure 9. To address this limitation, we would like to extend our method to use instance-level information as well. Additionally, we would like to develop methods which do not require labels from the target domain.

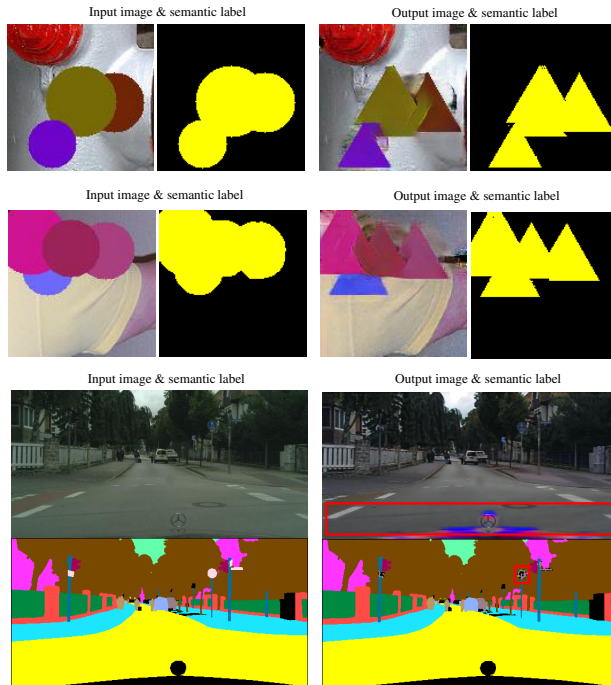


Figure 9: Typical failure cases of our approach. Top: in the multi circle to triangle task SemGAN cannot establish a foreground/background relationship between the objects. Center: Again in the object transfiguration task, SemGAN does not properly assign the colors of the foreground objects. The classes, in this case, are preserved. Bottom: In the Cityscape \rightarrow GTA domain translation task the network introduces artifacts in the image (top red box). SemGAN also fails to preserve the stop sign class. We note that this network was only trained for 66 epochs (out of 200) and these artifacts might be due to short training time. We will include updated figures in the final version of this paper.

References

- [1] J.-Y. Zhu, T. Park, P. Isola, and A. A. Efros, “Unpaired Image-to-Image Translation Using Cycle-Consistent Adversarial Networks,” in *2017 IEEE International Conference on Computer Vision (ICCV)*, (Venice), pp. 2242–2251, IEEE, Oct. 2017. [1](#), [2](#), [3](#), [4](#), [5](#), [6](#), [8](#)
- [2] D. Eigen and R. Fergus, “Predicting Depth, Surface Normals and Semantic Labels with a Common Multi-scale Convolutional Architecture,” in *2015 IEEE International Conference on Computer Vision (ICCV)*, (Santiago, Chile), pp. 2650–2658, IEEE, Dec. 2015. [1](#), [2](#)
- [3] W. Xian, P. Sangkloy, V. Agrawal, A. Raj, J. Lu, C. Fang, F. Yu, and J. Hays, “TextureGAN: Controlling Deep Image Synthesis with Texture Patches,” in *2018 IEEE/CVF Conference on Computer Vision and Pattern Recognition*, (Salt Lake City, UT), pp. 8456–8465, IEEE, June 2018. [1](#), [2](#)
- [4] R. Zhang, P. Isola, and A. A. Efros, “Colorful Image Colorization,” in *ECCV*, 2016. [1](#)
- [5] C. Ledig, L. Theis, F. Huszar, J. Caballero, A. Cunningham, A. Acosta, A. Aitken, A. Tejani, J. Totz, Z. Wang, and W. Shi, “Photo-Realistic Single Image Super-Resolution Using a Generative Adversarial Network,” in *2017 IEEE Conference on Computer Vision and Pattern Recognition (CVPR)*, (Honolulu, HI), pp. 105–114, IEEE, July 2017. [1](#)
- [6] P. Isola, J.-Y. Zhu, T. Zhou, and A. A. Efros, “Image-to-Image Translation with Conditional Adversarial Networks,” *CoRR*, vol. abs/1611.07004, 2016. [1](#), [2](#), [5](#)
- [7] T.-C. Wang, M.-Y. Liu, J.-Y. Zhu, G. Liu, A. Tao, J. Kautz, and B. Catanzaro, “Video-to-Video Synthesis,” *CoRR*, vol. abs/1808.06601, 2018. [1](#), [2](#)
- [8] I. Goodfellow, J. Pouget-Abadie, M. Mirza, B. Xu, D. Warde-Farley, S. Ozair, A. Courville, and Y. Bengio, “Generative Adversarial Nets,” in *Advances in Neural Information Processing Systems 27* (Z. Ghahramani, M. Welling, C. Cortes, N. D. Lawrence, and K. Q. Weinberger, eds.), pp. 2672–2680, Curran Associates, Inc., 2014. [1](#), [2](#), [3](#)
- [9] Z. Yi, H. Zhang, P. Tan, and M. Gong, “DualGAN: Unsupervised Dual Learning for Image-To-Image Translation,” in *The IEEE International Conference on Computer Vision (ICCV)*, Oct. 2017. [1](#), [2](#)
- [10] M. Tomei, M. Cornia, L. Baraldi, and R. Cucchiara, “Art2real: Unfolding the Reality of Artworks via Semantically-Aware Image-to-Image Translation,” *CoRR*, vol. abs/1811.10666, 2018. [1](#)
- [11] L. Karacan, Z. Akata, A. Erdem, and E. Erdem, “Learning to Generate Images of Outdoor Scenes from Attributes and Semantic Layouts,” *CoRR*, vol. abs/1612.00215, 2016. [1](#)
- [12] T.-C. Wang, M.-Y. Liu, J.-Y. Zhu, A. Tao, J. Kautz, and B. Catanzaro, “High-Resolution Image Synthesis and Semantic Manipulation with Conditional GANs,” in *Proceedings of the IEEE Conference on Computer Vision and Pattern Recognition*, 2018. [1](#)
- [13] Y. Taigman, A. Polyak, and L. Wolf, “Unsupervised Cross-Domain Image Generation,” *arXiv:1611.02200 [cs]*, Nov. 2016. [arXiv: 1611.02200](#). [2](#), [4](#)
- [14] A. Gonzalez-Garcia, J. van de Weijer, and Y. Bengio, “Image-to-image translation for cross-domain disentanglement,” in *Advances in Neural Information Processing Systems 31* (S. Bengio, H. Wallach, H. Larochelle, K. Grauman, N. Cesa-Bianchi, and R. Garnett, eds.), pp. 1287–1298, Curran Associates, Inc., 2018. [2](#)
- [15] S. Benaim and L. Wolf, “One-Sided Unsupervised Domain Mapping,” in *NIPS*, 2017. [2](#)
- [16] R. Zhang, T. Pfister, and J. Li, “Harmonic Unpaired Image-to-image Translation,” in *International Conference on Learning Representations*, 2019. [2](#)
- [17] M. Amodio and S. Krishnaswamy, “TraVeLGAN: Image-to-image Translation by Transformation Vector Learning,” *arXiv preprint arXiv:1902.09631*, 2019. [2](#)

- [18] P. Li, X. Liang, D. Jia, and E. P. Xing, "Semantic-aware Grad-GAN for Virtual-to-Real Urban Scene Adaption," *CoRR*, vol. abs/1801.01726, 2018. [2](#)
- [19] P. Z. Ramirez, A. Tonioni, and L. d. Stefano, "Exploiting Semantics in Adversarial Training for Image-Level Domain Adaptation," *CoRR*, vol. abs/1810.05852, 2018. [2](#)
- [20] J. Hoffman, E. Tzeng, T. Park, J.-Y. Zhu, P. Isola, K. Saenko, A. A. Efros, and T. Darrell, "Cycada: Cycle-consistent adversarial domain adaptation," *arXiv preprint arXiv:1711.03213*, 2017. [2, 3](#)
- [21] A. Cherian and A. Sullivan, "Sem-GAN: Semantically-Consistent Image-to-Image Translation," *CoRR*, vol. abs/1807.04409, 2018. [2](#)
- [22] X. Liang, H. Zhang, and E. P. Xing, "Generative Semantic Manipulation with Contrasting GAN," *CoRR*, vol. abs/1708.00315, 2017. [2](#)
- [23] Y. Alami Mejjati, C. Richardt, J. Tompkin, D. Cosker, and K. I. Kim, "Unsupervised Attention-guided Image-to-Image Translation," in *Advances in Neural Information Processing Systems 31* (S. Bengio, H. Wallach, H. Larochelle, K. Grauman, N. Cesa-Bianchi, and R. Garnett, eds.), pp. 3693–3703, Curran Associates, Inc., 2018. [2](#)
- [24] S. Mo, M. Cho, and J. Shin, "Instance-aware Image-to-Image Translation," in *International Conference on Learning Representations*, 2019. [2, 5, 6](#)
- [25] Z. Murez, S. Kolouri, D. J. Kriegman, R. Ramamoorthi, and K. Kim, "Image to Image Translation for Domain Adaptation," *CoRR*, vol. abs/1712.00479, 2017. [3](#)
- [26] W. Hong, Z. Wang, M. Yang, and J. Yuan, "Conditional Generative Adversarial Network for Structured Domain Adaptation," in *2018 IEEE/CVF Conference on Computer Vision and Pattern Recognition*, (Salt Lake City, UT), pp. 1335–1344, IEEE, June 2018. [3](#)
- [27] W. Zhang, W. Ouyang, W. Li, and D. Xu, "Collaborative and Adversarial Network for Unsupervised Domain Adaptation," in *2018 IEEE/CVF Conference on Computer Vision and Pattern Recognition*, (Salt Lake City, UT), pp. 3801–3809, IEEE, June 2018. [3](#)
- [28] J. Shen, Y. Qu, W. Zhang, and Y. Yu, "Wasserstein distance guided representation learning for domain adaptation," *arXiv preprint arXiv:1707.01217*, 2017. [3](#)
- [29] E. T. Hassan, X. Chen, and D. J. Crandall, "Unsupervised Domain Adaptation using Generative Models and Self-ensembling," *CoRR*, vol. abs/1812.00479, 2018. [3](#)
- [30] M. Long, Z. CAO, J. Wang, and M. I. Jordan, "Conditional Adversarial Domain Adaptation," in *Advances in Neural Information Processing Systems 31* (S. Bengio, H. Wallach, H. Larochelle, K. Grauman, N. Cesa-Bianchi, and R. Garnett, eds.), pp. 1640–1650, Curran Associates, Inc., 2018. [3](#)
- [31] E. Hosseini-Asl, Y. Zhou, C. Xiong, and R. Socher, "Augmented Cyclic Adversarial Learning for Low Resource Domain Adaptation," in *International Conference on Learning Representations*, 2019. [3](#)
- [32] A. Paszke, S. Gross, S. Chintala, G. Chanan, E. Yang, Z. DeVito, Z. Lin, A. Desmaison, L. Antiga, and A. Lerer, "Automatic differentiation in PyTorch," in *NIPS-W*, 2017. [5](#)
- [33] T.-Y. Lin, M. Maire, S. Belongie, J. Hays, P. Perona, D. Ramanan, P. Dollár, and C. L. Zitnick, "Microsoft coco: Common objects in context," in *European conference on computer vision*, pp. 740–755, Springer, 2014. [6](#)
- [34] S. R. Richter, V. Vineet, S. Roth, and V. Koltun, "Playing for Data: Ground Truth from Computer Games," *CoRR*, vol. abs/1608.02192, 2016. [6](#)
- [35] M. Cordts, M. Omran, S. Ramos, T. Rehfeld, M. Enzweiler, R. Benenson, U. Franke, S. Roth, and B. Schiele, "The Cityscapes Dataset for Semantic Urban Scene Understanding," *CoRR*, vol. abs/1604.01685, 2016. [6, 7](#)
- [36] O. Ronneberger, P. Fischer, and T. Brox, "U-net: Convolutional networks for biomedical image segmentation," in *International Conference on Medical image computing and computer-assisted intervention*, pp. 234–241, Springer, 2015. [7](#)

Supplementary Material

Here, we present additional qualitative results and comparisons on previously introduced datasets. The rest of the appendix is organized as follows. First, we provide more details about the images used to perform the experiments. Next, we discuss a simple extension of the CycleGAN generator and discriminator with an additional channel for the semantic labels. Through examples in multiple datasets, we illustrate the deficiencies of such an approach and the importance of the cross-entropy loss in Appendix B. Finally, we present additional qualitative results for experiments that were introduced in the paper. Specifically, we present additional results for the GTA \leftrightarrow Cityscapes, object transfiguration on our shapes dataset and translation between images of different animals from the COCO dataset.

A Resolution of the Images Used in Performed Experiments

Due to resource constraints, we relied on down-sampled versions of the original datasets for training. Specifically, we used image size 256×512 pixels for the GTA \leftrightarrow Cityscapes experiments, image size 128×128 pixels for the shape transformation experiments and image size 256×256 pixels for the anecdotal animal transformation experiments.

B Deficiencies of CycleGAN Extension with Additional Channel & Importance of Cross Domain Loss



Figure 10: Qualitative analysis of the effects of our proposed cross domain loss. In absence of the cross domain loss, the generator is free to change the semantic labels in different spatial regions of the target image (two middle columns). With the addition of cross domain loss such anomalies can be prevented (last two columns).

The cross-domain loss introduced in our paper, is critical to preserving the underlying semantics of a scene. Without the cross-domain loss, the generator is free to change the semantic labels in different spatial regions of the target image. We show such an example in Figure 10. CycleGAN can be extended with an additional channel to handle semantic information. However, this extension cannot use the additional semantic information and suffers from similar visual artifacts as the original algorithm. We illustrate the deficiencies of this design with a few examples in Figure 11.

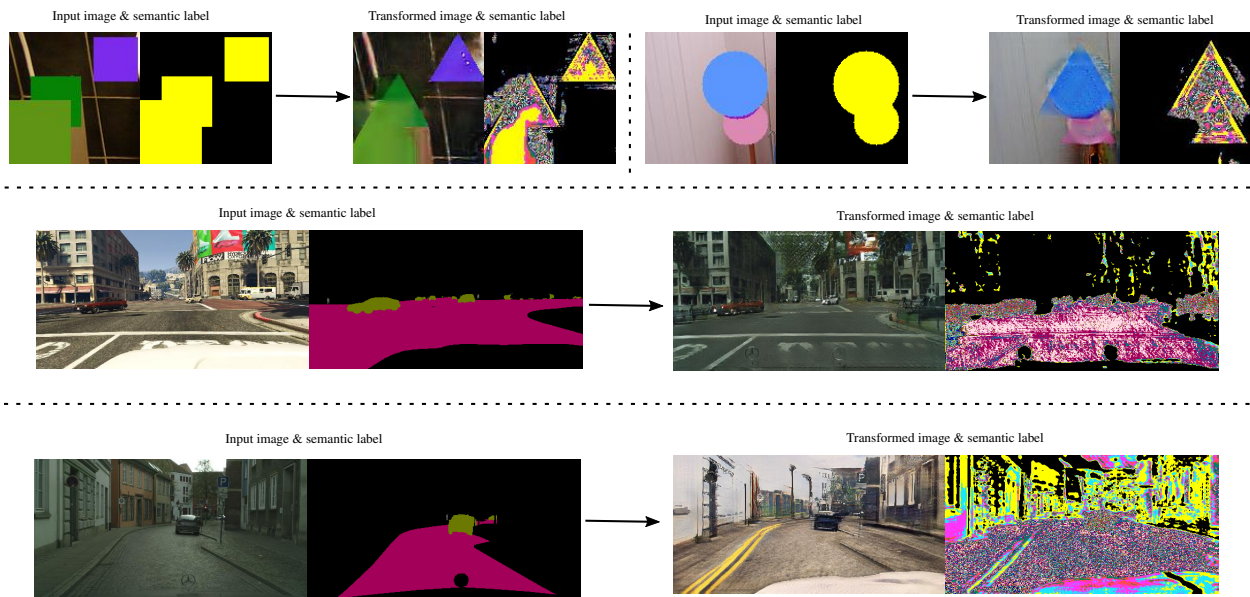


Figure 11: The trivial extension of adding an extra channel in CycleGAN results in erroneous semantic translations. The network generates values between 0 – 255 for both the target image and its mask, it generates arbitrary semantic labels for both binary (top row: translation from square to triangle/ circle to triangle) and multi-class (middle row: GTA → Cityscape, bottom row: Cityscape → GTA) test cases. Additionally, this technique is incapable of using the extra information available from the semantic labels and it produces similar visual artifacts like CycleGAN itself. Note that, for the GTA ↔ Cityscapes examples in the figure, only four classes were used (people, road, car and ignore label).

C Additional Results



Figure 12: Domain transfer: GTA \rightarrow CityScape. We show the performance of CycleGAN and our network. CycleGAN does not preserve the underlying geometry and creates visual artifacts due to switches in class labels.

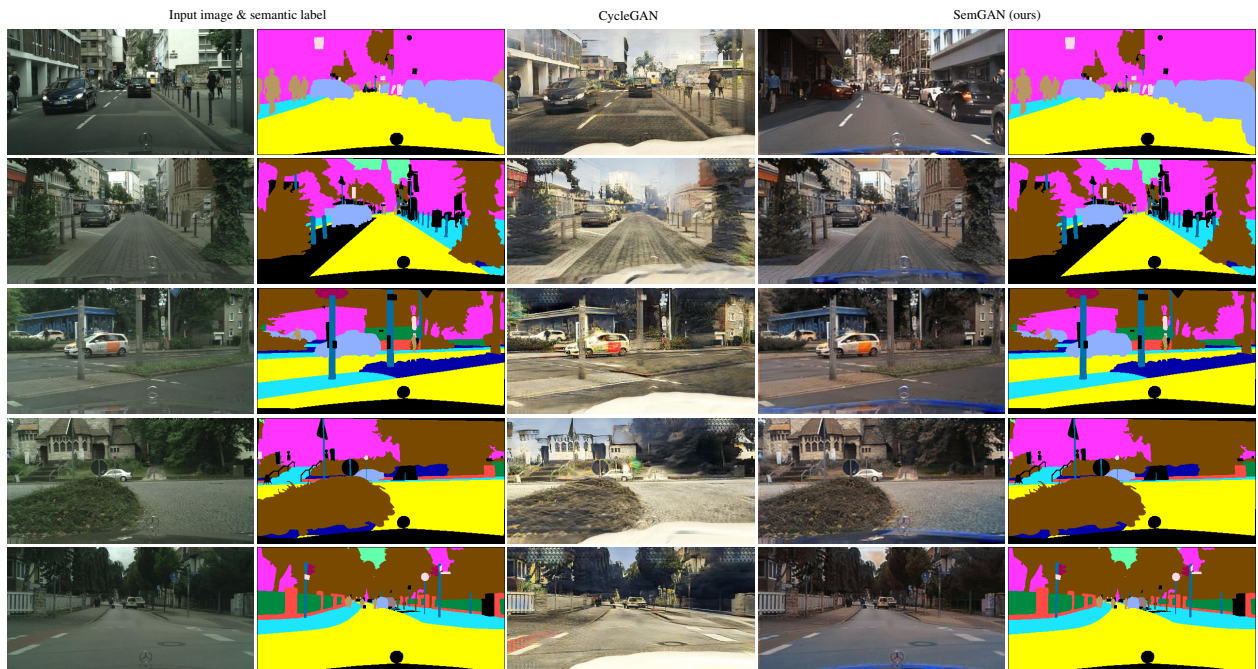
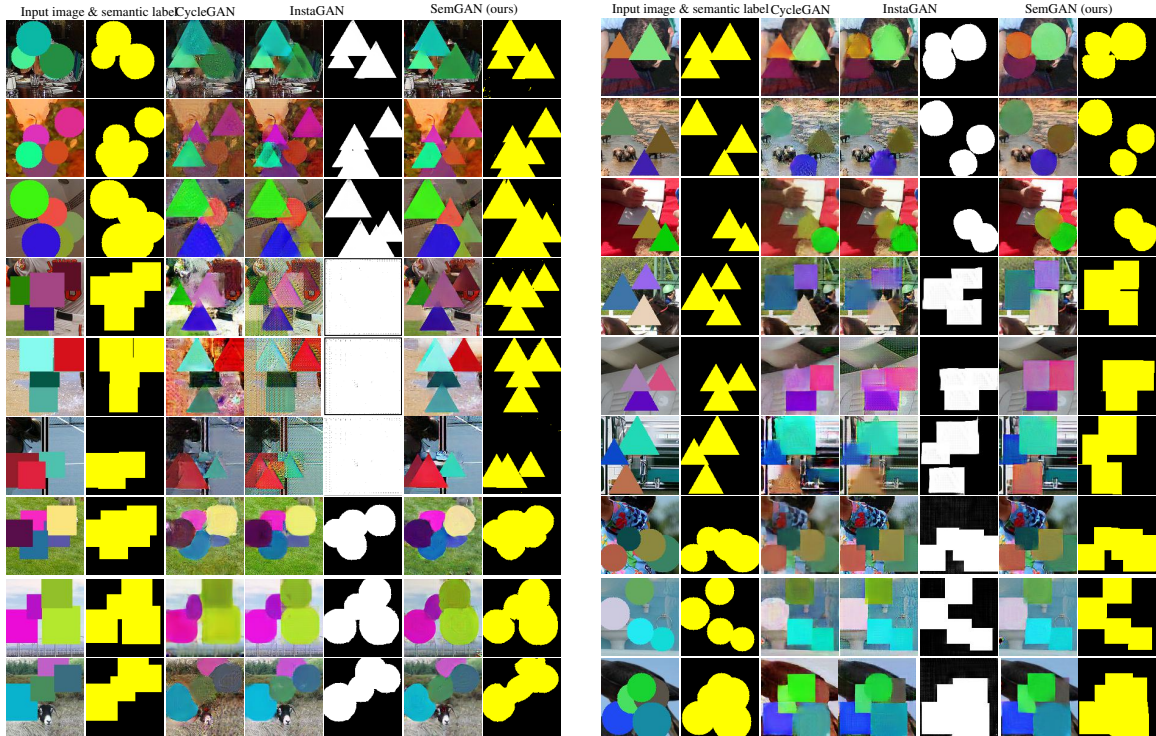


Figure 13: Additional examples of domain transfer from CityScape \rightarrow GTA. Similar to Figure 12, we compare the performance of CycleGAN and our network. Again, CycleGAN does not preserve the underlying geometry and creates visual artifacts due to switches in class labels.



(a) Top three rows: Transforming circles into triangles, center three rows: Squares into triangles and bottom three rows: Squares into circles.

(b) Top three rows: Transforming triangles into circles, center three rows: Triangles into squares and bottom three rows: Circles into squares.

Figure 14: We show additional qualitative comparison of CycleGAN, InstaGAN and our method. We can see that our method transforms foreground objects in a more concise way. InstaGAN translation of the label masks in the Squares \rightarrow Triangle case (center rows) leads to mode collapse. CycleGAN suffers from visual artifacts. CycleGAN and InstaGAN both struggle when the network has to generate object contours that are larger than the original objects (triangle to squares).

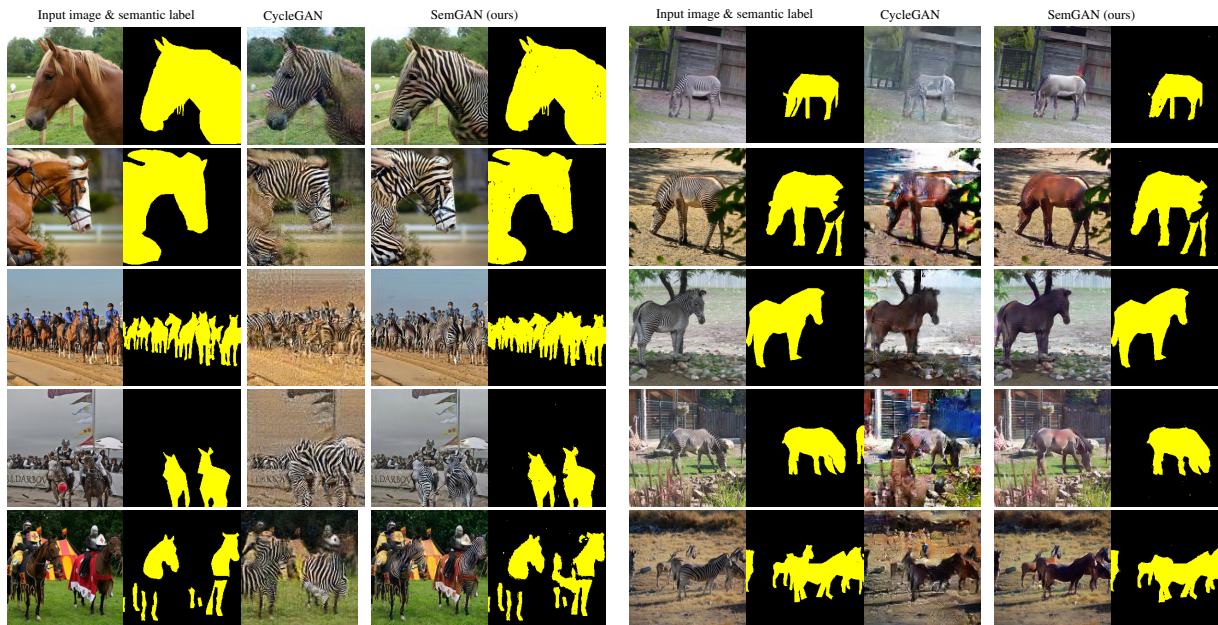


Figure 15: Additional results on Horse \leftrightarrow Zebra. Left: Horse \rightarrow Zebra. Right: Zebra \rightarrow Horse. As noted in the paper, adding a label preserving loss aids the preservation of background and the translations of color, texture and geometry of the foreground object.

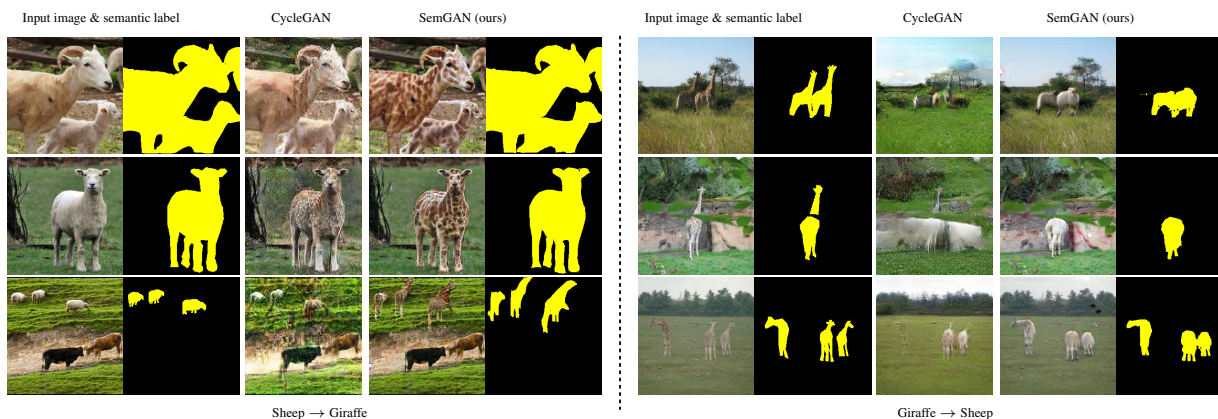


Figure 16: Additional results on Sheep \leftrightarrow Giraffe.

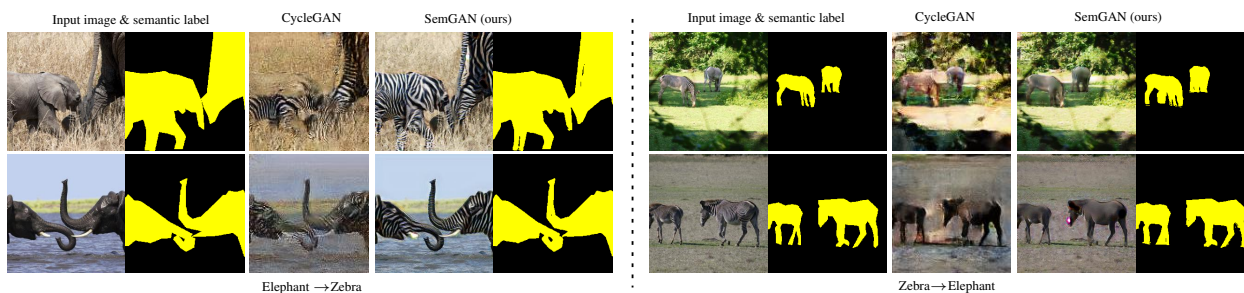


Figure 17: Additional results on Elephant \leftrightarrow Zebra